Journal of Earthquake and Tsunami (JET)

Tsunami current inundation of ground with coastal vegetation effects; an initial step towards a natural solution for tsunami amelioration

N. A. K. Nandasena[1)], Norio Tanaka[2), *] and Katsutoshi Tanimoto[2)]

1) Department of Civil Engineering, University of Moratuwa, Katubedda, Sri Lanka
2) Graduate School of Science and Engineering, Saitama University, Japan
255 Shimo-Okubo, Sakura-ku, Saitama-shi, Saitama-ken 338-8570, Japan

*Corresponding Author: Graduate School of Science and Engineering, Saitama University, Japan, 255 Shimo-Okubo, Sakura-ku, Saitama-shi, Saitama-ken 338-8570, Japan
e-mail: tanaka01@mail.saitama-u.ac.jp, tel/fax: +81-48-858-3564

Abstract

A densely grown coastal vegetation belt of *Pandanus odoratissimus* to reduce the tsunami energy was quantitatively analyzed by an enhanced one-dimensional numerical model that included variations of topography and tsunami characteristics. The drag and inertia forces were assumed as the total resistance generated by the vegetation. A relatively small period tsunami wave was more destructive than a relatively large period tsunami wave of the same height, although densely grown vegetation effectively reduced the tsunami energy in the case of the small period tsunami wave. A very mild ground slope was more vulnerable to thrashing by tsunami waves than a relatively steep ground

slope. Moreover, densely growing coastal vegetation on the very mild ground slope dissipated tsunami energy more efficiently than the same vegetation on the relatively steep ground slope.

Key words: vegetation, numerical simulation, tsunami, topography

1. Introduction

Tsunamis are among the most dreadful natural disasters, and depending on their wave energy, they can cause immeasurable damage to both living creatures and physical property in the hinterland within a very short period. Previous studies have developed various innovative strategies to both minimize and prevent the extent of the destruction. Especially since the Indian Ocean tsunami in 2004, the ability of coastal vegetation to minimize the tsunami energy has been studied because the damage was significantly reduced in places behind relatively wide, densely grown vegetation belts compared with the damage in places having no vegetation (Kathiresan & Rajendran, 2005; Mascarenhas & Jayakumar, 2007). Post-tsunami field investigations, numerical simulations (depth-averaged shallow water wave approximations including resistance forces by the vegetation) and experimental studies (sinusoidal or bore wave front generations with the vegetation modeled by cylindrical rods or other substitutes) have been employed to elucidate the effect of coastal vegetation on tsunami energy reduction. Latief et al. (1999) and Harada & Imamura (2000) described the dynamic behavior of the tsunami flow as it passed through mangrove forests, and described the effectiveness of mangrove forests against the tsunami impact by experimental and numerical methods. Hirashi & Harada (2003) described the possibility of employing green belts for tsunami prevention based on a field survey. Furthermore, experimental studies were carried out by them to evaluate the effects of the green belt by comparing it with other possible coastal protection methods such as coastal dikes, rubble breakwaters, and a tsunami-protective house model. Harada & Imamura (2006) examined quantitatively the hydrodynamic effects of coastal forests on tsunami reduction and determined the limitations of vegetation. Tanaka et al. (2007) investigated the condition of trees after the 2004 Indian Ocean tsunami and

reported that densely grown costal vegetation species were more effective than sparsely grown coastal vegetations for tsunami energy reduction. Nandasena et al. (2007b) quantitatively estimated the reduction in tsunami energy by the selected dominant species investigated in Tanaka et al. (2007) with limited input conditions in a numerical simulation.

In order to design an effective landscape with coastal vegetation, more study is needed on a wide range of tsunami conditions and forest characteristics. Therefore, the objective of this study was to extend the quantitative evaluation of the effects of a densely grown vegetation type, *Pandanus odoratissimus* (hereafter, *P. odoratissimus*), which is dominant on South Asian coasts, on tsunami energy reduction and to include variations of topography and tsunami characteristics in an enhanced mathematical background.

2. Materials and methods

2.1 Mathematical background

Depth-averaged shallow water wave equations were used to simulate the propagation of tsunami waves in the near shore and over the ground. These equations (continuity and momentum), which have been retrofitted with the porosity term by which the volumetric effect of the vegetation is rectified, are as follows (Nandasena et al. 2007a, Nandasena et al. 2007b). These equations were solved in an explicit numerical scheme in which the staggered grid method in space and the leapfrog method in time were adopted. The numerical discretization is included in the appendix (A-1).

$$\theta_h \frac{\partial \zeta}{\partial t} + \frac{\partial Q_x}{\partial x} = 0 \tag{2.1}$$

$$\theta_h \frac{\partial Q_x}{\partial t} + \frac{\partial (\frac{Q_x^2}{h})}{\partial x} + \theta_h g h \frac{\partial h}{\partial x} + \theta_h^{3/2} g h \frac{\partial z}{\partial x} + \theta_b \sqrt{\theta_h} \frac{\tau_x}{\rho} + \frac{\theta_h^{3/2}}{\rho} \sum_{i=1}^{k} f_{xi} = 0 \tag{2.2}$$

where Q_x = discharge per unit width, ζ = water surface elevation, h = water depth, z = bed elevation measured from a selected datum, τ_x = bed resistance, $\sum_{i=1}^{k} f_{xi}$ = total resistance generated by the vegetation, g = gravitational acceleration, ρ = density of sea water (taken as 1024 kg/m^3), θ_h = depth-averaged porosity, θ_b = bed porosity ($0 < \theta_h, \theta_b < 1$), $\theta_h = 1 - m\frac{\pi b_h^2}{4}, \theta_b = 1 - m\frac{\pi b_b^2}{4}$, b_h = depth-averaged tree diameter for water depth h, b_b = equivalent tree diameter on the ground, and m = number of trees per unit area. In this study, total resistance by the vegetation is assumed by the sum of the drag and inertia components. The resistance forces and the bed resistance per unit area were reformulated to be compatible with equation (2.2) as follows.

Bed resistance:

$$\tau_x = \rho g n_0^2 Q_x^2 / (\theta_h h^{7/3}) \tag{2.3}$$

Drag force:

$$F_{dx} = m\rho \frac{1}{2} C_{d-all} b_{ref} h \frac{Q_x^2}{h^2 \theta_h} \tag{2.4}$$

where $C_{d-all} = C_{d-ref} \frac{1}{h} \int_0^h \frac{b(y)}{b_{ref}} \frac{C_d(y)}{C_{d-ref}} dy$

Inertia force:

$$F_{ix} = m\rho C_M \forall_{d.a.} \frac{d(Q_x / h\sqrt{\theta_h})}{dt} \tag{2.5}$$

where $\forall_{d.a.} = \frac{\pi}{4} b_{ref}{}^2 h \frac{1}{h} \int_0^h \frac{b(y)^2}{b_{ref}{}^2} dy$

where n_0 = Manning's roughness coefficient (=0.025 in this study, referring to Harada and Imamura (2006)), $C_{d\text{-}ref}$ = reference drag coefficient (=1.0 in this study), b_{ref} = reference diameter of a tree at 1.2 m above ground level, $b(y)$ = diameter of a tree at height y from the ground, $C_d(y)$ = coefficient of drag at height y from the ground, C_M =

inertia coefficient (=2.0 in this study), and $\forall_{d.a.}$ = depth averaged volume subjected to inertia force.

2.2 Numerical model validation

Existing field data / observations were not accurate enough to validate the numerical model. Thus, the numerical model was validated through a limited experimental study by Tanaka et al. (2008). They employed an experimental setup similar to one shown in Fig. 3(a) and (b). A range of wave gauges, out of which two were in front of and behind the vegetation model, was deployed to measure temporal variation of water surface elevations. Firstly the numerical model was calibrated with the case without vegetation model and Manning's roughness coefficient was found to be 0.025 for the bed slope. In turn, the numerical model was validated with the case with vegetation model and drag coefficient for the vegetation was about 1.5. Inertia effect was negligible. For more details, refer Tanaka et al. (2008).

2.3 Vegetation species' properties

Fig. 1 shows the vertical configuration and the drag characteristics of *P. odoratissimus* vegetation. The reference tree diameter, b_{ref} = 0.195 m, is measured at 1.2 m above ground level. The average tree height, aerial root height, and tree density are 8 m, 2 m, and 0.21 number of trees/m^2, respectively. (These values are for a mature tree based on the field investigations conducted in some coastal areas of Sri Lanka and Thailand.) As shown in Fig. 1, *P. odoratissimus* has a complex aerial root structure that provides additional stiffness to the drag coefficient; $C_d(y)$ varies from 1.5 to 1.0, and for additional drag by branches and leaves, $C_d(y)$ is taken as 1.25 (Tanaka et al. 2007).

2.4 Bathymetry and topography

Fig. 2 shows a schematic sketch of the model bed. The water depth is 200 m at the wave generation boundary. It continues for 5000 m and is connected to a 1:100 slope that spans

20000 m until it meets the shoreline. The horizontal distance from the shoreline to the vegetation front is 20 m. The rear boundary of the vegetation belt is changed with changing belt thickness.

2.5 Simulation scenarios and assumptions

Sinusoidal wave height, H_S, selected was 3.0 m at the wave generation boundary as shown in Fig.2. From the shoreline, three ground slopes were employed: 1:50 (relatively steep), 1:100 (average or typical), and 1:1000 (very mild). Two vegetation belts, 50 m (narrow) and 200 m (wide), were tested. Three tsunami wave periods, T_P, were selected: 10 min (relatively small), 20 min (average or typical), and 40 min (relatively large).

The bed profile is divided into three zones in a simulation perspective; the nonlinear convective term and the bed resistance term are not important in the linear zone as shown in Fig.2. However, the effects of the above terms are pertinent in the nonlinear zone; hence, the effects of these terms are considered in the nonlinear zone. A transition zone, in which a smooth change of the equation (equation 2.2) from linear to nonlinear occurs, merges the linear and nonlinear zones. Discretization sizes were Δx = 5 m and Δt = 0.056 s. Numerical simulations were performed until the first tsunami wave fully inundated the land area and then complete withdrawal occurred.

The following assumptions were made in the numerical simulation. The dynamic nature of the vegetation (shaking, bending of trunk and branches) in a tsunami force was neglected. The wave height was selected to ensure that the vegetation did not break, because the breaking phenomenon is more complex and the facts are still obscure (Tanaka et al., 2008). The tsunami was a sinusoidal wave and non-reflective at the wave generation boundary. The inertia coefficient was constant, and the drag coefficient was changed with the vegetation characteristics based upon studies in the literature, as explained in Section 2.2. An infinitely long vegetation belt perpendicular to the tsunami direction is assumed in the one-dimension numerical simulation. Thus, the results explained below overestimate the reality because it is hard to find very long vegetation belts in the practice, but, even if it were so, this would lead to a quantitative comparison

study for understanding the correlations between the ground slope, the tsunami period, and the dense coastal vegetation from the disaster-mitigation point of view.

2.6 Experimental study

The scale of 1:100 was used for the experimental study, and the details of the vegetation model are shown in Fig. 3(a). *P. odoratissimus* tree has complex lateral variations, but here a depth-averaged diameter with the tree height was used for simplicity. The vegetation model was arranged in a staggered system, and the vegetation model width was 1 m in the wave direction. Fig. 3(b) shows the vegetation model fixed on a bed slope model inside the flume. The bed slope model was made of wooden planks. It has two steep slopes, 1:4.7 and 1:20.5. The water depth in front of the wave paddle was 44 cm. An electric wave generator was used to synthesize sinusoidal long waves at a period of 20 s. Two capacitance-type wave gauges (G1 and G2) were deployed in front of and behind the vegetation model. The water surface elevation was measured at 5 Hz frequency for with and without vegetation models.

3. Results and discussions

A ratio is defined as follows to understand the effectiveness of the coastal vegetation to hamper the tsunami energy as a percentage change of wave parameters with reference to the without vegetation.

$$Percentage\ change = \frac{(with\ vegetation - without\ vegetation)}{without\ vegetation}\% \qquad (2.6)$$

This ratio reflects a decrement in a hydraulic property by a negative percentage or an increment in a hydraulic property by a positive percentage due to the vegetation effect. Respective combinations were analyzed to explore the vegetation effect on the topography and tsunami wave characteristics in order to dissipate tsunami energy.

3.1 Numerical modeling results - Ground slope effect

Figs. 4 and 5 show the temporal variations in water depth and current velocity in front of and behind the 50 m wide vegetation belt on 1:50 and 1:1000 ground slopes respectively, while Table 1 explains the percentage changes in the maximum water depth and the maximum current velocity in front of and behind the vegetation belts of 50 m and 200 m, with reference to that without vegetation.

3.1.1 Percentage change of hydraulic characteristics

The reduction of the water depth behind the vegetation on the 1:50 ground slope for both 50 m and 200 m belts was negligible in comparison with the case without vegetation. This indicates that the capacity of vegetation to reduce the water depth is minimal for the relatively steep slope. However, when the ground slope gradually decreases, the reduction in water depth behind the vegetation belt is increased. According to the results shown in Table 1, percentages of the maximum water depth reduction behind the 50 m vegetation belt were 2.8%, 8.2%, and 19% for 1:50, 1:100, and 1:1000 ground slopes. In addition, it is clear that widening the vegetation belt definitely increased the reduction of the maximum water depth behind the vegetation belt. Ostensibly, the maximum water depth in front of the vegetation would be larger in comparison with the case without vegetation, which is inferred from the wave reflection. In fact, the wave reflection is dominant in front of the vegetation on the very mild ground slope, as shown in Fig. 5. When the ground slope gradually becomes steeper, the reflection phenomenon gradually decreases. However, in spite of the wave reflection that occurs in the cases of 1:50 and 1:100 ground slopes, the maximum water depth in front of the vegetation belt is a little less than that without vegetation (Table 1). This seemed to be a strange phenomenon, and thus the experimental study explained in 2.6 was incorporated to substantiate the results derived by the numerical simulations.

The experimental results reveal that the maximum water surface elevation in front of the vegetation model was less than the maximum water surface elevation measured without vegetation for a steep ground slope, such as that shown in Fig. 6. This indicates

that the results derived from the numerical simulations for the densely grown vegetation on the relatively steep ground slope, which were assumed to be strange earlier, are realistic. The authors assume that this was a combined effect of the relatively steep slope and the densely growing vegetation.

The percentage reduction of the maximum current velocity was higher than the percentage reduction of the maximum water depth behind the vegetation belt irrespective of the ground slope and the width of the vegetation belt. When the ground slope was increased, the percentage reduction of the maximum current velocity (landwards) behind the vegetation was amplified. For the 50 m belt, the maximum current velocity reductions were 26%, 33.8%, and 37.1% for 1:1000, 1:100, and 1:50 respectively, which is the opposite of the maximum water depth reduction trend. Nonetheless, the difference was not very large. The maximum current velocity shoreward was extremely reduced behind the vegetation belt on the very mild slope (1:1000), and it took a considerable time to retrieve sea water from the ground behind the vegetation area. This resulted in a feeble ground slope effect to accelerate the offshore flow, and a flow-path contraction due to the dense vegetation. Perhaps the water depth on the ground would remain the same, like an inundation, until the next killer wave came to the ground, as shown in Fig. 5. Such phenomena have been reported by tsunami survivors. It is interesting to point out that the maximum current velocity shoreward in front of the vegetation on the relatively steep slope was increased by 33.3% and 45.6% for the 50 m and 200 m vegetation belts compared to the case without vegetation. This is attributed to the resultant hydrostatic pressure difference at the front boundary, whereas for the ground slopes of 1:100 and 1:1000, the maximum current velocities shoreward were reduced at the same location in comparison with the case without vegetation, as shown in Table 1.

A destructive hydraulic force generated by a tsunami flow on structures can be roughly calculated by multiplication of sea water density, water depth, and the square of the current velocity (Hatori 1984). In this calculation, it was assumed that the total hydraulic force acts on the structure (i.e., the structure is taller than the tsunami water depth) and the current velocity become zero after striking the structure. Dense coastal vegetation can remarkably reduce the damage force behind the vegetation belt on the very mild slope. In fact, the percentage reductions of the maximum hydraulic force

behind the 50 m belt on 1:50, 1:100, and 1:1000 ground slopes were 35.6%, 42%, and 50.2%, respectively.

It was obvious that a larger horizontal run-up was observed on the very mild slope than on the relatively steep slope due to the reduction of gravity resistance. The percentage reductions of the horizontal run-up by the 50 m vegetation belt on 1:50 (relatively steep), 1:100 (typical), and 1:1000 (very mild) were about 0%, 10%, and 19%. Similar reductions for the 200 m belt were about 1.7%, 18.9%, and 34.1% in this study. This confirmed that the effectiveness of the horizontal run-up reduction was increased by the vegetation with the decrement of the ground slope. The tsunami delay times for the 50 m vegetation belt on all slopes were the same, 6s, but for the 200 m belt, it was increased to 44s, 48s, and 50s from the very mild to the relatively steep slope. However, the difference was not significant.

Based on the numerical simulation results, employing densely grown coastal vegetation on the very mild ground slope dissipates tsunami energy more efficiently than the same vegetation on the steep ground slope. The tsunami period effect is discussed in the next section, in which the optimal combination for tsunami energy dissipation (i.e., densely grown vegetation on the very mild slope) was employed.

3.2 Numerical modeling results - Tsunami period effect

Fig. 7 illustrates the spatial variation of the water depth and the current velocity through the vegetation belt when the tsunami front moved in the landward direction.

3.2.1 Percentage change of hydraulic characteristics

It can be observed that the wave reflection was dominant at the vegetation front for the relatively small tsunami wave period (10 min). However, despite the tsunami wave period, the wave reflection could be observed in front of the dense vegetation on the very mild ground slope. In comparison, the tsunami wave with a relatively small period accompanied a higher current velocity than the relatively large period tsunami wave of the same wave height, as shown in Fig 7.

From the results in Table 2 and illustrated by Fig. 7, it is possible to understand that the wave period of a tsunami is one of the factors that determines the extent of the damage to the structures behind the vegetation. A relatively small period tsunami can impose a massive force in a shorter period compared to the relatively large period tsunami with the same wave height in the case without vegetation. It is interesting that the vegetation belt can remarkably reduce the damage force due to the small period tsunami wave compared to the relatively large period wave.

It is noticed in the numerical results that the tsunami of T_p = 40 min achieves the largest horizontal run-up, and T_p = 20 min and T_p = 10 min are reduced in order. This implies that a tsunami with a relatively large period can displace a larger amount of water to the ground than the relatively small period wave. Thus, the tsunami period is one of factors that control the horizontal run-up on the ground for the same wave height. The percentage of horizontal run-up reductions by the 50 m vegetation belt for the tsunami periods of 10 min, 20 min, and 40 min were 19%, 18%, and 19%. Similar results for the 200 m belt were 35%, 34%, and 33% in comparison with the case without vegetation. The tsunami delay times due to the 50 m belt of vegetation for T_p = 10 min, 20 min, and 40 min are 4 s, 6 s, and 6 s. Similar results for the 200 m belt are 37 s, 45 s, and 57 s.

4. Conclusions

The conclusions derived from this study are related to considerably long vegetation belts (cross-stream direction) than for vegetation patches because the one-dimension numerical simulation assumes an infinitely long vegetation belt perpendicular to the wave direction.

The wave reflection was dominant in front of densely grown vegetation on the very mild slope, and the magnitude was increased with increasing belt thickness in the tsunami direction. Regardless of the tsunami wave period, the wave reflection was observed in front of the vegetation on the very mild ground slope. When the tsunami period was increased, the reflection phenomenon was gradually decreased for the same incident wave height.

The relatively small period tsunami wave was more destructive than the relatively large period tsunami wave of the same wave height, whereas the vegetation effectively reduced the tsunami energy in the case of the small period wave.

The shoreward current velocities were significantly reduced compared to the landward current velocities on the very mild slope due to the vegetation effect.

The effectiveness of the horizontal run-up reduction due to the vegetation was increased with the decrement of the ground slope.

The very mild ground slope was more vulnerable to thrashing by the tsunami waves than the relatively steep ground slope, but the densely grown coastal vegetation on the very mild ground slope was more efficient in dissipating tsunami energy in comparison with the same vegetation on the steep ground slope condition.

Appendix A-1

An explicit numerical scheme, staggered in space and leapfrogged in time.

Continuity equation:

$$\theta_{h\,i+1/2}^{\,n-1}\left[\frac{\varsigma_{i+1/2}^{n}-\varsigma_{i+1/2}^{n-1}}{\Delta t}\right]+\left[\frac{Q_{x\,i+1}^{\,n-1/2}-Q_{x\,i}^{\,n-1/2}}{\Delta x}\right]=0$$

Momentum equation:

$$\theta_{h\,i}^{\,n}\left[\frac{Q_{x\,i}^{\,n+1/2}-Q_{x\,i}^{\,n-1/2}}{\Delta t}\right]+\frac{1}{\Delta x}\left[\vartheta_1\frac{Q_{x\,i-1}^{\,n-1/2\,2}}{h_{i-1}^{n}}+\vartheta_2\frac{Q_{x\,i}^{\,n-1/2\,2}}{h_{i}^{n}}+\vartheta_3\frac{Q_{x\,i+1}^{\,n-1/2\,2}}{h_{i+1}^{n}}\right]+\theta_{h\,i}^{\,n}gh_i^n\left[\frac{h_{i+1/2}^{n}-h_{i-1/2}^{n}}{\Delta x}\right]$$

$$+(\theta_{h\,i}^{\,n})^{3/2}gh_i^n\left[\frac{z_{i+1/2}^{n}-z_{i-1/2}^{n}}{\Delta x}\right]+gn_0^2\frac{\theta_b}{\sqrt{\theta_{h\,i}^{\,n}}}\frac{\left|Q_{x\,i}^{\,n-1/2}\right|}{h_i^{n\,7/3}}\left[\frac{\left[Q_{x\,i}^{\,n+1/2}+Q_{x\,i}^{\,n-1/2}\right]}{2}\right]$$

$$+\frac{1}{2}mC_{d-ref}b_{ref}\overline{\alpha\beta}_{\,i}^{\,n}\sqrt{\theta_{h\,i}^{\,n}}\frac{\left|Q_{x\,i}^{\,n-1/2}\right|}{h_i^n}\left[\frac{\left[Q_{x\,i}^{\,n+1/2}+Q_{x\,i}^{\,n-1/2}\right]}{2}\right]$$

$$+mC_M \frac{\pi}{4} b_{ref}{}^2 \overline{\alpha^2}{}_i^n \theta_{hi}{}^n h_i^n \left[\frac{\left[\frac{Q_{xi}{}^{n+1/2}}{h_i^n} - \frac{Q_{xi}{}^{n-1/2}}{h_i^{n-1/2}} \right]}{\Delta t} \right] = 0$$

The upwind scheme is used for non-linear convective terms in order to preserve the numerical stability. If $Q_{xi}{}^{n-1/2} \geq 0$, then $\vartheta_1 = -1, \quad \vartheta_2 = 1, \quad \vartheta_3 = 0$ or else $\vartheta_1 = 0, \quad \vartheta_2 = -1, \quad \vartheta_3 = 1$. A semi Crank-Nicholson scheme is used for bed roughness and drag terms. If the properties at time intervals *n* and *n-1/2* are known, $\varsigma_{i+1/2}^n$ and $Q_{xi}{}^{n+1/2}$, the unknowns can be calculated.

$$\overline{\alpha\beta} = \frac{1}{h} \int_0^h \frac{b(y)}{b_{ref}} \frac{C_d(y)}{C_{d-ref}} dy$$

$$\overline{\alpha^2} = \frac{1}{h} \int_0^h \frac{b(y)^2}{b_{ref}{}^2} dy$$

References

Harada, K., and Imamura, F. [2000] "Experimental study on the resistance by mangrove under the unsteady flow," *Proc. of the 1st Congress of the Asian and Pacific Coastal Engineering*, Dalian, Chaina, pp. 975–984.

Harada, K., and Imamura, F. [2006] "Effects of coastal forest on tsunami hazard mitigation – A preliminary investigation," *Tsunamis: Case Studies and Recent Development*, ed. K. Satake (Advances in natural and Technological Hazards Research, Springer), pp. 279–292.

Hatori, T. [1984] "On the damage to houses due to tsunamis" (In Japanese), *Bull. Earthquake Research Inst. Univ. Tokyo* **59**, 433–439.

Hiraishi, T. and Harada, K. [2003] "Greenbelt tsunami prevention in South-Pacific region," *Report of the Port and Airport Research Institute*, Vol. **4**2, No. 2.

Kathiresan, K., and Rajendran, N. [2005] "Coastal mangrove forests mitigated tsunami, Short note", *Estuarine, Coastal and Shelf Science* **65**, 601–606.

Latief, H., Harada, K., and Imamura, F. [1999] "Experimental and numerical study on the effect of mangrove to reduce tsunami," *Tohoku Journal of Natural Disaster Science* **35**, 127–132.

Mascarenhas, A., Jayakumar, S. [2007] "An environmental perspective of the post-tsunami scenario along the coast of Tamil Nadu, India: Role of sand dunes and forests," *Environmental Management* - In press.

Nandasena, N. A. K., Tanaka, N., and Takagi, T. [2007a] "A new derivation of horizontal two dimensional depth averaged momentum equation and continuity equation, which include total effect of porosity inside the vegetation," *Annual Journal of Hydraulic Engineering, JSCE* **52**, 163-168.

Nandasena, N. A. K., Tanaka, N., and Tanimoto K. [2007b] "Capability of coastal vegetation species dominant in Asian region to retardate the tsunami impact," *proc. of the 9th International Summer Symposium, JSCE*, Japan, pp.115-118.

Tanaka, N., Sasaki, Y., Mowjood M.I.M., and Jinadasa, K.B.S.N. [2007] "Coastal vegetation structures and their functions in tsunami protection: Experience of the recent Indian Ocean tsunami," *Landscape and Ecological Engineering* **3**, 33-45.

Tanaka, N., Nandasena, N. A. K., Jinadasa, K. S. B. N., Sasaki, Y., Tanimoto, K. and Mowjood, M. I. M. [2008] "Developing Effective Bioshield for Tsunami Protection," Civil and Environmental Engineering Systems – in press.

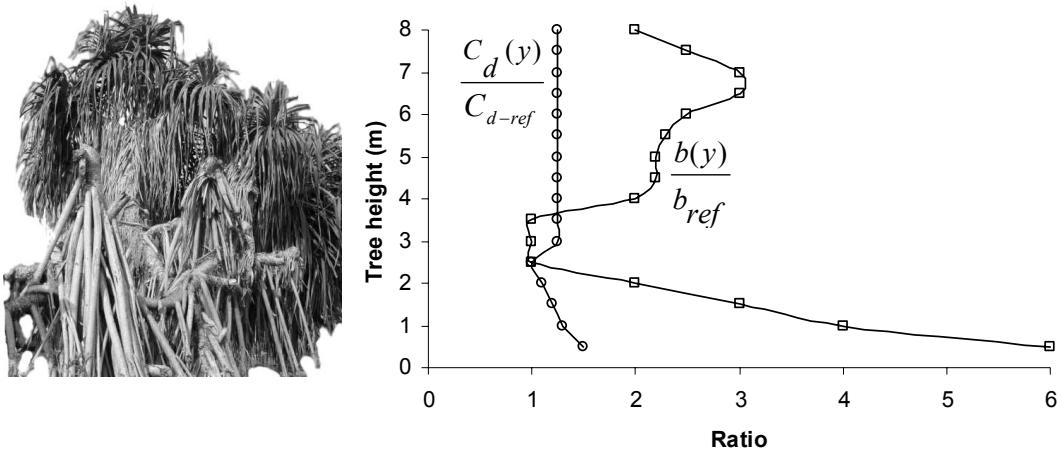

Fig. 1 Vertical configuration and drag characteristics of *P. odoratissimus*

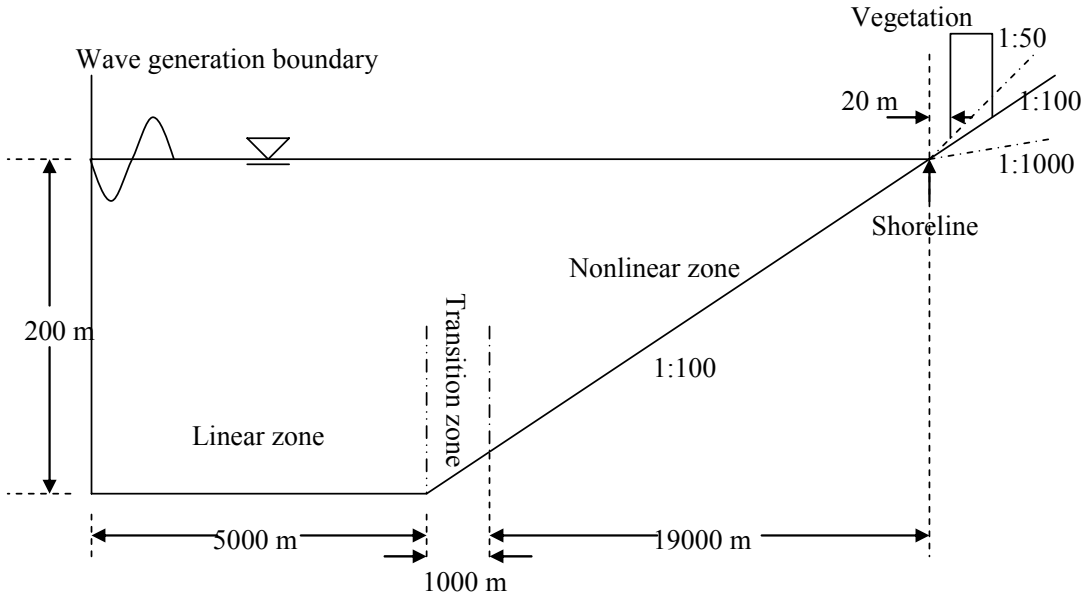

Fig. 2 Cross section of bathymetry and topography

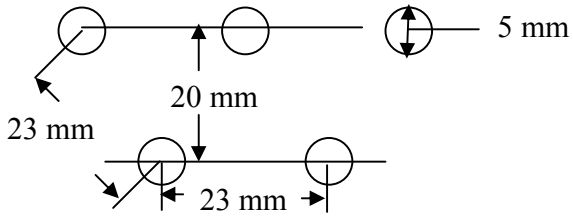

Fig. 3(a) Details of vegetation model.

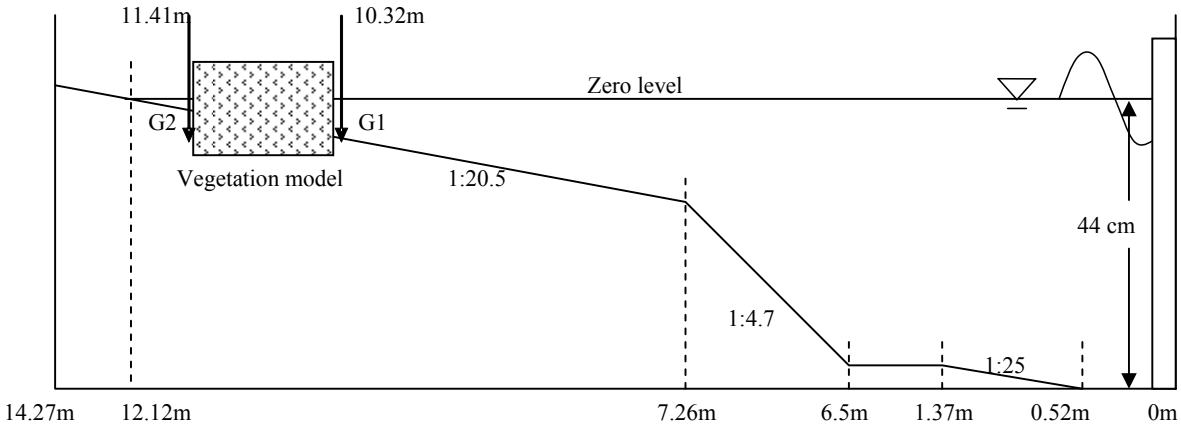

Fig. 3(b) Experimental setup, not to scale.

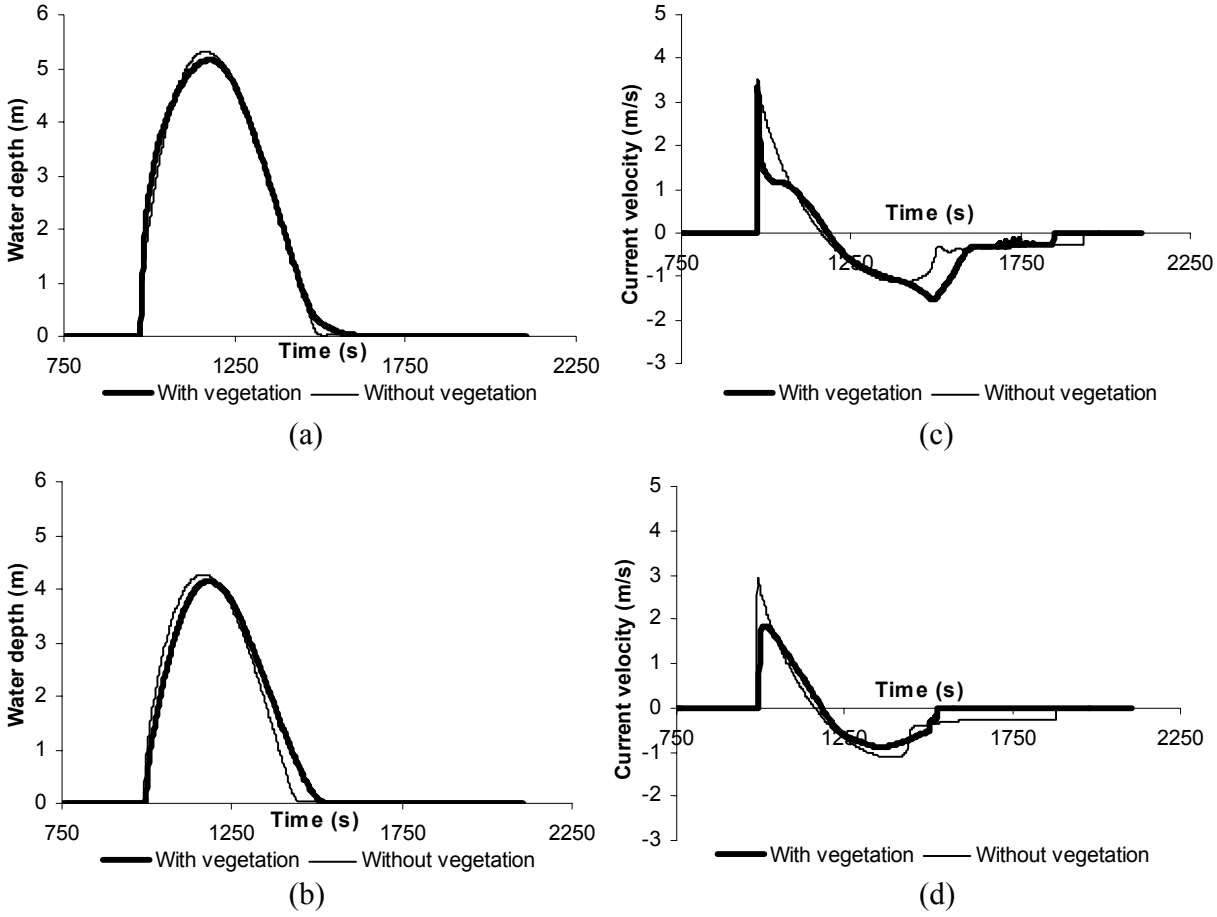

Fig. 4. Temporal variation of water depth (a) in front of and (b) behind the vegetation, and temporal variation of current velocity (c) in front of and (d) behind the vegetation. The vegetation belt width is 50 m. Ground slope is 1:50 (relatively steep) from the shoreline. H_s = 3 m and T_p = 20 min.

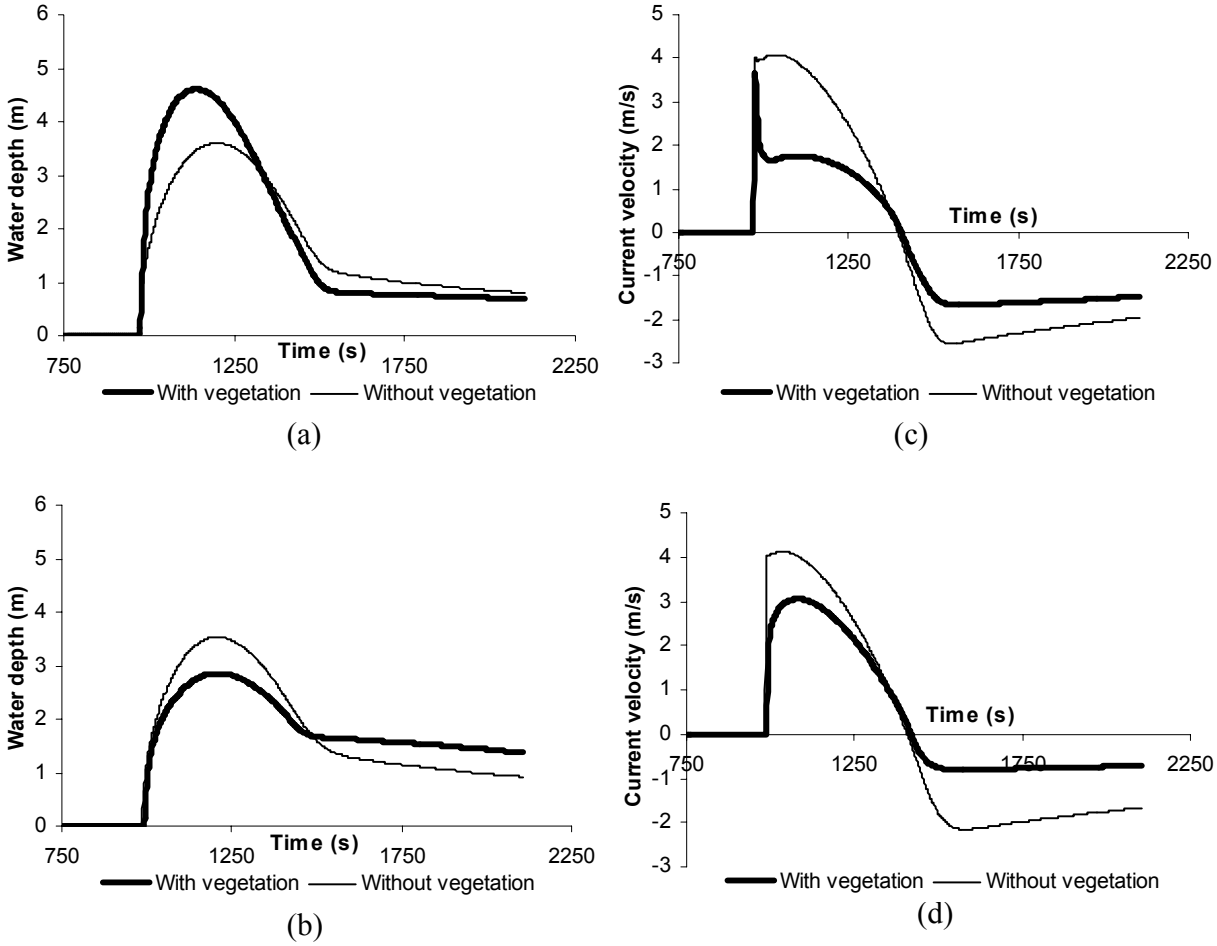

Fig. 5. Temporal variation of water depth (a) in front of and (b) behind the vegetation, and temporal variation of current velocity (c) in front of and (d) behind the vegetation. The vegetation belt width is 50 m. Ground slope is 1:1000 (very mild) from the shoreline. H_s = 3 m and T_p = 20 min.

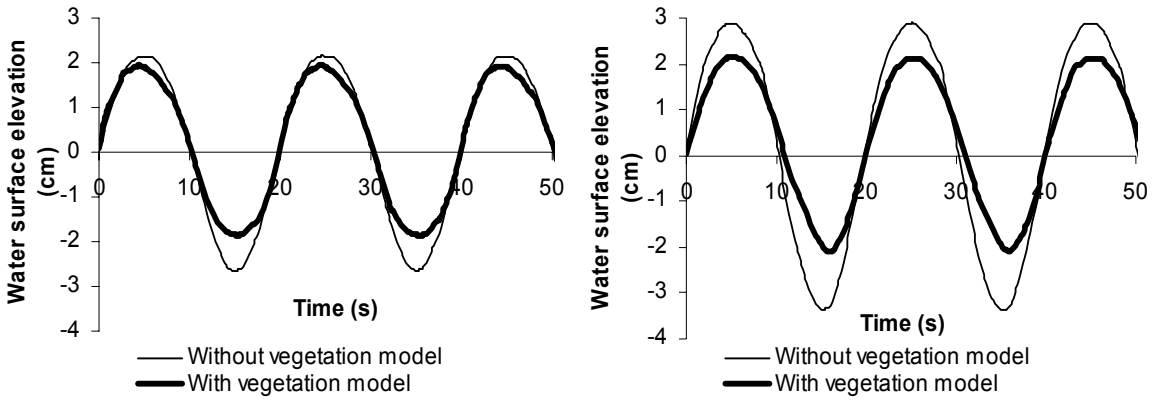

(a) (b)

Fig. 6 Temporal variation of water surface elevation (a) in front of (G1) and (b) behind (G2) the vegetation model (Experimental study).

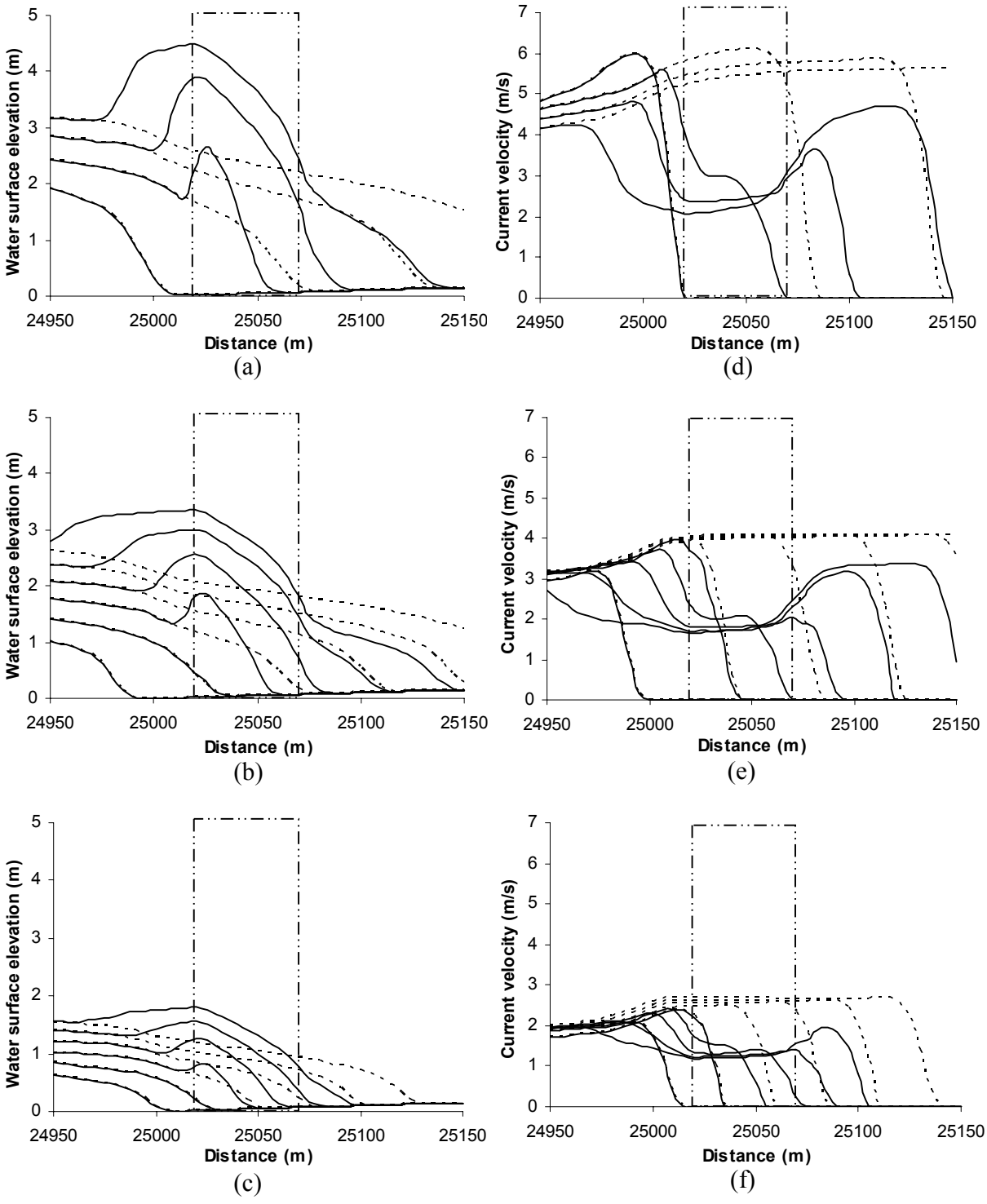

Fig. 7. Spatial variation of water depth for tsunami periods of (a) 10 min, (b) 20 min, and (c) 40 min and corresponding spatial current velocity variation for tsunami periods (d) 10 min, (e) 20 min, and (f) 40 min. The vegetation region (50 m) is shown by a rectangle, and solid lines indicate results with vegetation, while dashed lines illustrate results without vegetation. H_s = 3 m, and ground slope is 1:1000 from the shoreline. The time lag between two consecutive contours is 10s.

Table 1. Percentage change of maximum water depth and maximum current velocity in front of and behind the vegetation on different ground slopes. Percentage change is expressed in comparison with the case without vegetation, as defined by equation (2.6).

Ground slope	Belt width (m)	Condition	Front			Behind		
			MWD (m)	MCV (m/s)		MWD (m)	MCV (m/s)	
				LW	OW		LW	OW
1:50	50	WOV	5.31	3.54	1.14	4.27	2.94	1.13
		WV	5.15	3.34	1.52	4.15	1.85	0.88
		PC	-3.0%	-5.6%	33.3%	-2.8%	-37.1%	-22.1%
	200	WOV	5.31	3.54	1.14	1.42	1.48	0.83
		WV	5.12	3.34	1.66	1.26	0.94	0.46
		PC	-3.6%	-5.6%	45.6%	-11.0%	-36.5%	-44.6%
1:100	50	WOV	5.07	3.8	2.75	4.61	3.55	2.64
		WV	4.84	3.52	2.41	4.23	2.35	-1.38
		PC	-4.5%	-7.4%	-12.4%	-8.2%	-33.8%	-47.7%
	200	WOV	5.07	3.8	2.75	3.36	3.08	2.3
		WV	5.1	3.52	2.14	2.53	1.72	-0.74
		PC	0.6%	-7.4%	-22.2%	-25%	-44.2%	-67.8%
1:1000	50	WOV	3.6	4.08	2.57	3.53	4.12	2.16
		WV	4.61	3.68	1.66	2.85	3.05	0.81
		PC	28.1%	-9.8%	-35.4%	-19.0%	-26.0%	-62.5%
	200	WOV	3.6	4.08	2.57	3.33	4.16	1.76
		WV	5.05	3.68	1.27	2.09	2.56	0.4
		PC	40.3%	-9.8%	-50.6%	-37.0%	-38.5%	-77.3%

WOV - without vegetation, WV - with vegetation, PC - percentage change, MWD - maximum water depth, MCV - maximum current velocity, LW - landward direction, and OW - offshoreward direction. H_s = 3 m and ground slope is 1:1000 from the shoreline.

Table 2. Percentage change of maximum water depth and maximum current velocity in front of and behind the vegetation due to different tsunami periods. Percentage change is expressed in comparison with the case without vegetation, as defined by equation (2.6).

Tsunami period (min)	Belt width (m)	Condition	Front			Behind		
			MWD (m)	MCV (m/s)		MWD (m)	MCV (m/s)	
				LW	OW		LW	OW
10	50	WOV	3.21	6.32	2.2	3.11	5.99	1.82
		WV	4.92	5.7	1.41	2.65	3.52	0.68
		PC	53.3%	-9.8%	-35.9%	-15.0%	-41.2%	-62.6%
	200	WOV	3.21	6.32	2.2	2.87	5.6	1.47
		WV	5.21	5.7	1.2	1.83	2.73	0.33
		PC	62.3%	-9.8%	-45.5%	-36.0%	-51.3%	-77.6%
20	50	WOV	3.6	4.08	2.57	3.53	4.12	2.16
		WV	4.61	3.68	1.66	2.85	3.05	0.81
		PC	28.1%	-9.8%	-35.4%	-19.0%	-26.0%	-62.5%
	200	WOV	3.6	4.08	2.57	3.33	4.16	1.76
		WV	5.05	3.68	1.27	2.09	2.56	0.4
		PC	40.3%	-9.8%	-50.6%	-37.0%	-38.5%	-77.3%
40	50	WOV	3.67	2.99	2.78	3.61	2.99	2.36
		WV	4.05	2.23	1.85	2.94	2.36	0.91
		PC	10.4%	-25.4%	-33.5%	-19.0%	-21.1%	61.4%
	200	WOV	3.67	2.99	2.78	3.45	2.99	1.95
		WV	4.35	2.23	1.37	2.21	2.02	0.45
		PC	18.5%	-25.4%	-50.7%	-36.0%	-32.4%	-76.9%

WOV - without vegetation, WV - with vegetation, PC - percentage change, MWD - maximum water depth, MCV - maximum current velocity, LW - landward direction, and OW - offshoreward direction. H_s = 3 m and ground slope is 1:1000 from the shoreline.